Eur. Phys. J. Special Topics **224**, 415–424 (2015)

DOI: 10.1140/epjst/e2015-02370-6

THE EUROPEAN PHYSICAL JOURNAL SPECIAL TOPICS

Regular Article

Interfacial instability of a condensing vapor bubble in a subcooled liquid

I. Ueno[1,2,a], J. Ando[1], Y. Koiwa[1], T. Saiki[1], and T. Kaneko[1,2]

[1] Dept. Mechanical Engineering, Fac. Science & Technology, Tokyo University of Science, Chiba, Japan
[2] Research Institute for Science & Technology (RIST), Tokyo University of Science, Chiba, Japan

Received 31 July 2014 / Received in final form 16 February 2015
Published online 8 April 2015

Abstract. A special attention is paid to the condensing and collapsing processes of vapor bubble injected into a subcooled pool. We try to extract the vapor-liquid interaction by employing a vapor generator that supplies vapor to the subcooled pool through an orifice instead of using a immersed heating surface to realize vapor bubbles by boiling phenomenon. This system enables ones to detect a spatio-temporal behavior of a single bubble of superheated vapor exposed to a subcooled liquid. In the present study, vapor of water is injected through an orifice at constant flow rate to the subcooled pool of water at the designated degree of subcooling under the atmospheric pressure. The degree of subcooling of the pool is ranged from 0 K to 70 K, and the vapor temperature is kept constant at 101 °C. The behaviors of the injected vapor are captured by high-speed camera at frame rate up to 0.3 million frame per second (fps) to track the temporal variation of the vapor bubble shape. It is found that the abrupt collapse of the vapor bubble exposed to the subcooled pool takes place under the condition that the degree of subcooling is greater than around 30 K, and that the abrupt collapse always takes place accompanying the fine disturbances or instability emerged on the free surface. We then evaluate a temporal variation of the apparent 'volume' of the bubble V under the assumption of the axisymmetric shape of the vapor bubble. It is also found that the instability emerges slightly after the volume of the vapor bubble reaches the maximum value. It is evaluated that the second derivative of the corresponding 'radius' R of the vapor bubble is negative when the instability appears on the bubble surface, where $R = \sqrt[3]{\frac{3V}{4\pi}}$. We also illustrate that the wave number of the instability on the liquid-vapor interface increases as the degree of subcooling.

1 Introduction

Removal of a vigorous amount of heat generated in a narrow area has been severer and more critical issue for thermal managements of facilities/devices. Cloud networking

[a] e-mail: ich@rs.tus.ac.jp

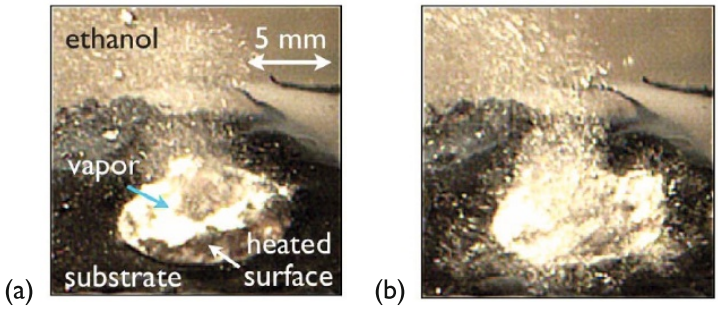

Fig. 1. Example of microbubble emission boiling known as MEB: (a) before and (b) after the onset of the MEB. Test fluid: ethanol, heated surface: copper of 10 mm in diameter, and $\Delta T_{\mathrm{sub}} = 50\,\mathrm{K}$ under atmospheric pressure. Finer vapor bubbles are radially emitted from the heated surface after the onset of the MEB. The original movie was given to the authors by courtesy of Prof. Koichi Suzuki at Tokyo University of Science, Yamaguchi.

systems handling huge amount of data, fuel cells in automobiles, facilities and devices for long-term exploration in severe environments such as a space are the sources of the amount of the heat to be cooled efficiently. High-performance CPU and GPU have been significant sources of the heat in the laptops, cell phones and any mobile electric devices. It is indispensable to overcome these problems in order to realize stable operations of such facilities/devices. Boiling phenomenon accompanying with a removal of the heat via latent heat from the heat source has been a potential candidate to be applied to such systems. In the recent decades, "microbubble emission boiling," known as the MEB, has been focused to solve severe issues aforementioned. It has been noticed that a higher heat flux than the critical heat flux (CHF) is realized under a certain degree of the subcooling [1–3]. Figure 1 indicates a typical example of the MEB; finer vapor bubbles are radially emitted from the heated surface after the onset of the MEB. Such an continuous emission of vapor bubbles results in keeping high heat transfer coefficient because of a continuous departure of vapor bubbles around the heating surface and supply of ambient liquid to the heating surface. This would bring invaluable impact to apply this powerful phenomenon to the devices even under microgravity conditions; in the case of the conventional pool boiling, vapor bubbles would stay near a heated surface, which results in seriously worse heat transfer coefficient and would result in fatal burnout in the system concerned.

Inada et al. [1] introduced this unique phenomenon, and researches have followed to accumulate valuable information on its occurring condition and heat transfer characteristics in the boiling on the flat surface [2,4–6], on the thin wire [7], and in the mini- and micro-channels [7,8]. These researches have indicated that this boiling process emerges under a rather high subcooled condition accompanying with continuous formation and emission of a number of micrometer-scale bubbles from the heated surface [3]. A series of experimental works were carried out by a group of The University of Tokyo to firstly illustrate growing and collapsing process of the vapor bubble on a thin wire [7]. Such a behavior of the vapor bubble is also observed in the MEB on the circular heating surface (Fig. 2). In this geometry, it has been known that cloud of the vapor bubbles almost covers the heating surface [5,6], and vigorously vibrate at almost constant frequency. The dynamics of the MEB itself, however, has not been fully understood at all to the best of our knowledge. One of the reasons for this comes from interactions among vapor bubbles, and those among liquid, vapor, and solid phases. Condensation process must be an essential phenomenon to enhance the heat transfer by supplying the ambient subcooled liquid to the heating surface. It has been noticed that it is quite difficult to detect a clear signature from

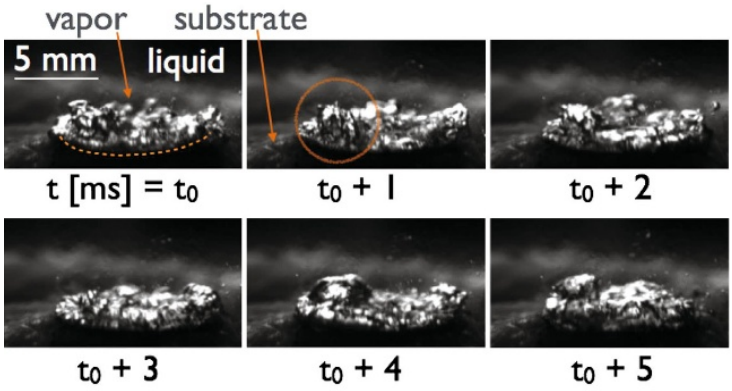

Fig. 2. Vapor bubble behaviors in the MEB on the circular heating surface. Images were taken via a high-speed camera from slightly obliquely above, and dashed line indicates the edge of the heating surface on the near side. One can see that the vapor bubbles violently grow and collapse on the periphery of the heating surface (circle). Test fluid is distilled water, and heating surface is made of copper whose diameter is of 10 mm. $\Delta T_{\mathrm{sub}} = 20\,\mathrm{K}$ under atmospheric pressure, and shutter speed: 0.1 ms. Experimental apparatus is described in Saiki et al. [6].

such complex processes over the heating plates under conditions of higher heat flux. Knowledge on bubble behaviors and corresponding heat transfer in the subcooled pool boiling has been accumulated by a series of fine experiments with array of the micro-scale heaters by using FC-72 [9,10] and water [11]. But the condensation processes under a higher heat flux have not been realized because the total output of the heat is strictly limited in the system employed. Disturbances on the vapor bubble in growing and bouncing processes were beautifully demonstrated as the fission of bubble in the explosive boiling of a droplet by Frost & Sturtevant [12]. Such a vigorous variation of the vapor bubble interface was explained by considering the Rayleigh-Taylor-like instability over the curved interface of the inertially growing vapor bubble [13]; the bubble dynamics was described with spherical harmonics, and indicated the occurring condition of the bubble fission as $\ddot{R} \geq 0$ as referred to the beginning of the rebound, where R indicates the radius of the vapor bubble, and $\ddot{R}$ indicates the second derivative with respect to time. On the bubble dynamics considering the condensing process of the vapor bubble and accompanying behaviors, however, almost no discussion has been made. Our group has focused on the condensing processes of a vapor bubble in a subcooled pool by employing a vapor injection system through the orifice [14,15]. Such a system enables us to extract the vapor-liquid interaction, which is hardly detected in a complex boiling under higher heat flux. We employ a vapor generator to supply vapor at designated flow rate to the subcooled pool instead of using an immersed heated surface for the boiling experiment. A spatio-temporal behavior of a single bubble of superheated vapor exposed to a subcooled liquid through this system is discussed in the present study. We especially focus on dynamic behaviors and instability arisen over the free surface of the condensing/collapsing vapor bubble by a high-speed observation system.

2 Experiment

Figure 3 illustrates the schematics of the apparatus. Experimental apparatus consists of three major components; the vapor generator and supplier, the subcooled pool, and

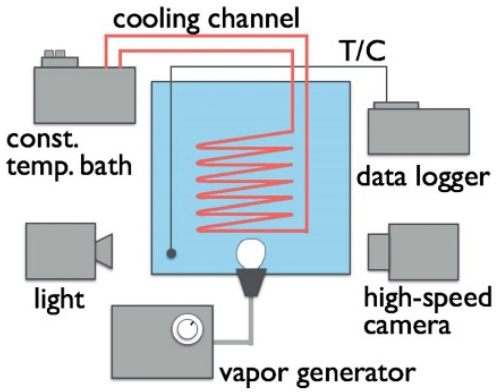

Fig. 3. Schematics of experimental apparatus.

the measuring system. The experimental system is almost the same as introduced by our group [14,15]. The vapor of the distilled water is produced in a closed chamber with an immersed heater as the vapor generator. The generated vapor is supplied to a subcooled pool filled with the same distilled water through a stainless-steel tube of 2.0 mm in inner diameter. The injection tube is immersed in the plate made of the PDMS (Polydimethylsiloxane) to realize the vapor injection through an "orifice." The plate with the injection tube is installed on the bottom wall of the tank for the subcooled pool. The supplying rate of the vapor is controlled by the valve on the vapor generator. The valve is located at the exit of the vapor-generation tank, and the volume of the channel between the valve and the tip of the orifice is of 2.6×10^4 mm^3. Temperature of the injected vapor is confirmed to keep almost constant at 101 °C through the series of the experiments. The tank for the subcooled pool is made of Pyrex® glass, and its inner width, depth and height are of 280 mm, 280 mm and 200 mm, respectively. The tank is opened to the atmosphere. The vapor supplying rate $Q_{\rm in}$ is defined here as an averaged flow rate of the vapor from the vapor generator to the orifice; the time series of the volume of the vapor is evaluated by measuring the volume variation of the vapor bubble injected to the saturated pool, that is, without any condensation of the vapor bubble formed in the pool. In the series of the present experiments, we set the supplying rate of the vapor from the vapor generator to the injection part $Q_{\rm in}$ of 56 mm^3/ms. This flow rate corresponds to the averaged vapor velocity through the orifice $V_{\rm in} \sim 17.8$ m/s. Noted that we have examined the vapor supplying rate up to 130 mm^3/ms in the preliminary experiments. In the case of $Q_{\rm in} > 100$ mm^3/ms we have found that the interface of the vapor bubble is not smooth anymore even under the saturated condition due to the Kelvin-Helmholtz instability; the relative velocity of the vapor and the ambient water results in disturbances over the interface, whose wavelength becomes of the order of $O(1$ mm). In order to focus on the disturbances due to the phase change process, we limit ourselves to carry out the experiments with the flow rate aforementioned. The thermal condition of the pooled fluid, or the degree of subcooling $\Delta T_{\rm sub} = T_{\rm sat} - T_\infty$, is controlled with cooling channel made of copper immersed in the pool, where $T_{\rm sat}$ and T_∞ indicate the saturation temperature under the pressure concerned and the ambient temperature, respectively. We measure the spatial distribution of the temperature in the pool with thermocouple (T/C) in the preliminary experiments as shown in Fig. 4 [15]. In the present study, the degree of subcooling is defined by use of the temperature at 20 mm apart from the orifice edge as T_∞. We are convinced by ourselves that the bulk of the pool far enough from the orifice keeps designated temperature, and that the degree of subcooling $\Delta T_{\rm sub}$ is maintained as designated. The injected vapor bubble

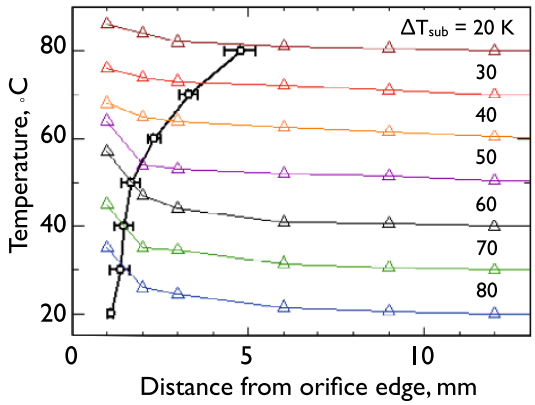

Fig. 4. Temperature distributions in the bulk pool above the orifice for different degree of subcooling ΔT_{sub} [15]. Circles in the figure indicate the farthest positions of the edge of the vapor bubble in the growing process under the designated ΔT_{sub}.

is captured by high-speed video camera at a frame rate up to 0.3 million fps with a back-lighting system.

3 Results & discussion

Figure 5 illustrates a typical example of growing and condensing processes of the injected vapor bubble into the subcooled pool. This figure indicates the result in the case of 40 K in the degree of subcooling. The instance shown in the first frame is referred as $t = t_0$. These successive images are captured from a single movie taken at 60,000 fps (frame per second) with a shutter speed of 1/72,080 s. It is noted that we extract images at the constant intervals from the original movie, so that the net frame rate becomes 1,250 fps. The injected vapor condenses with keeping rather smooth free surface even under such a large degree of subcooling of the pool. The vapor is continuously supplied to the bubble until the bubble departs from the orifice. After a while of growing stage, a necking process takes place on the bubble right above the orifice (at about $t = t_0 + 3.2$ ms in this case) accompanying with a condensation near its neck part; this is driven by the fluid flow induced by the growth and departure of the bubble from the orifice. The bubble detaches from the orifice, and drastically decreases its volume. This is explained by considering that the bubble is exposed to the subcooled pool without supplying the vapor to the bubble when the bubble is isolated. Tiny bubbles of $O(\mu\mathrm{m})$ in diameter are formed in the collapsing process, which are seen as the black clouds at the top region in the last frame at $t = t_0 + 5.6$ ms. Let us focus on the collapsing behavior of the vapor bubble as shown in Fig. 5; the bubble keeps a rather smooth interface at the early stage of the condensation right after the necking process at $t = t_0 + 3.2$ ms. Tiny but significant disturbances of $O(100\ \mu\mathrm{m})$ in wavelength emerge in the top region of the bubble ($t = t_0 + 4.0$ ms), and the instability grows as time elapses ($t = t_0 + 4.8$ ms). It is found that abrupt collapse of the isolated vapor bubble exposed to the subcooled pool never takes place without fine disturbances over the free surface.

We carry out a rough evaluation of the volume of condensing bubble as indicated by [14,16] in order to make a comparison with the Rayleigh-Taylor-like instability [13], as well as to illustrate the occurring condition of the instability. The apparent 'volume' of the bubble is evaluated by extracting the bubble edge (or perimeter) along a horizontal pixel line in the obtained images, and integrating the dish

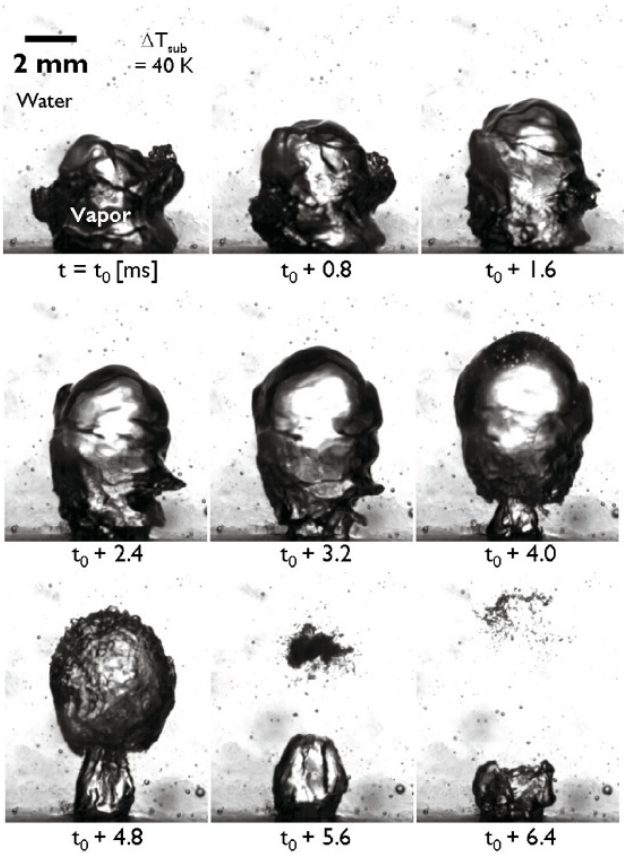

Fig. 5. Typical example of growing and condensing processes of the injected vapor bubble through the orifice into the pool of 40 K in the degree of subcooling. Scale bar in the first frame corresponds to 2.0 mm. Shutter speed is of 1/72,080 s.

along the vertical axis under an assumption that the bubble shape are axisymmetric. Figure 6 illustrates the condensing processes of the vapor bubble under various ΔT_{sub} in order to track the temporal variation of the vapor bubble size. Note that the volume is normalized by the maximum value $V_{\max}$ in each time series, and the instance when V reaches at $V_{\max}$ is defined as $t = 0$. In the case of $\Delta T_{\mathrm{sub}} = 20\,\mathrm{K}$, under which no disturbances emerge over the free surface in the condensing process, the volume decreases rather slowly, and no abrupt collapse takes place [6]. In the case of $\Delta T_{\mathrm{sub}} \geq 30\,\mathrm{K}$, on the other hand, the vapor bubble exhibits a different manner in the condensation. Enlarged view of the temporal variation of the bubble volume is illustrated in the frame (b). Note that the frame (b) does not involve the result in the case of $\Delta T_{\mathrm{sub}} = 20\,\mathrm{K}$. The scenario is described in the case of $\Delta T_{\mathrm{sub}} = 30\,\mathrm{K}$ for instance; the vapor bubble maintains its volume for a while (until $t \sim 0.3\,\mathrm{ms}$) after V reaches $V_{\max}$, and then drastically decreases its volume. At $t \sim 0.5\,\mathrm{ms}$ (see arrow in the frame (b)) defined as t_{d}, fine disturbances of rather short wavelength emerge on the bubble surface. The volume of the vapor bubble at $t = t_{\mathrm{d}}$ is defined as V_{d} hereafter. The condensing process is almost similar in quality under $\Delta T_{\mathrm{sub}} \geq 30\,\mathrm{K}$, but the time t_{d} becomes shorter as increasing ΔT_{sub}. We have to emphasize that such a disturbance emerged in the condensing vapor bubble is completely different from that observed in the rebounding bubble [12,13]. In the present case of vapor bubble collapse, it can be

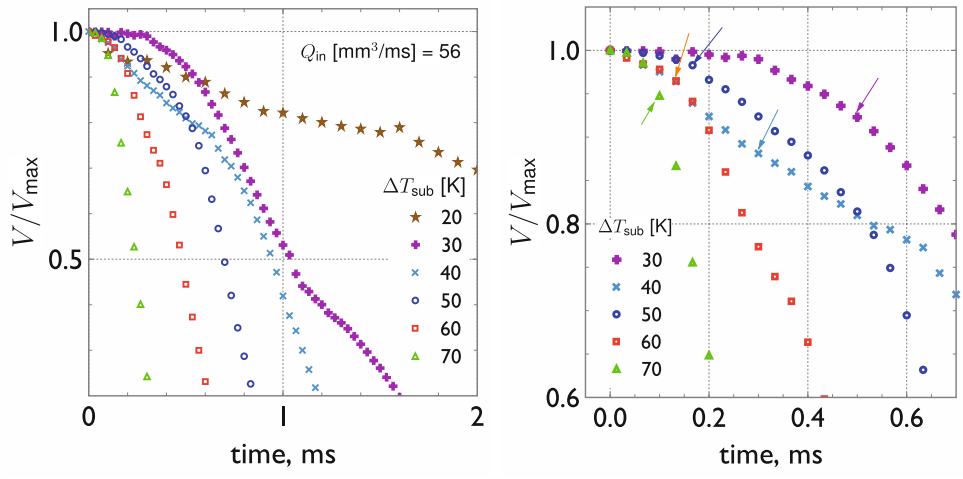

Fig. 6. Typical example of temporal variation of the vapor bubble volume in the condensing process; (a) long-range variations and (b) short-range variations except the data of $\Delta T_{\mathrm{sub}} = 20\,\mathrm{K}$ (under which no disturbances emerge in the condensing process). Arrows in the frame (b) indicate the instance when the disturbances appear on the vapor bubble surface. The volume is normalized by the maximum value of in each time series. Note that the data in the case of $\Delta T_{\mathrm{sub}} = 40\,\mathrm{K}$ does not correspond to those shown in Fig. 5.

translated from the variation of V that the instability arises under $\dot{R} < 0$ and $\ddot{R} < 0$, where R is the "corresponding radius" R to the evaluated volume V ($R = \sqrt[3]{\frac{3V}{4\pi}}$) of the vapor bubble. These results insist that the instability arises when the vapor bubble starts shrinking because of the condensation. And, the condition $\ddot{R} < 0$ implies the instability on the condensing vapor bubble is not the Rayleigh-Taylor type. It is of importance to evaluate the variation of the bubble volume as well as the period until the emergence of the disturbance as the trigger of the abrupt collapse in order to understand the correlation between the fine disturbances over the free surface and the bubble behaviors in the condensing process. The drop of the volume until the emergence of the disturbance is defined as $\Delta V = V_{\mathrm{max}} - V_{\mathrm{d}}$, and the time delay is defined as the period $\Delta t = t_{\mathrm{d}} - 0 = t_{\mathrm{d}}$, hereafter. The volume drop ΔV and the time delay against the degree of subcooling are illustrated in Figs. 7a and b, respectively. The dot indicates the average of the results from the seven different bubbles for each degree of subcooling, and the bar indicates the maximum and the minimum of the data set. It is noted that there exist no data under the $\Delta T_{\mathrm{sub}} = 20\,\mathrm{K}$ because no fine disturbances appear on the bubble surface. In the frame (a), the volume drop is rather high near the threshold of the fine disturbances over the vapor bubble, and decreases as the degree of subcooling. The time delay, in the frame (b), shows almost the same tendency. It should be noted that the evaluated "volume" involves uncertainties, because we assume the axisymmetric shape of the bubble in the evaluating process although the condensing bubble exhibits a complex shape. The physical message, however, might be explained by considering such tendencies in ΔV and its ratio to the V_{max}. That is, the condensation of about ten percent of the vapor inside the bubble triggers the formation of fine disturbances on the vapor bubble surface in about $0.1 \sim 0.5\,\mathrm{ms}$ resulting in the abrupt variation of the vapor bubble at last. Let us come back to the disturbances arisen on the vapor bubble. Zoomed view of the disturbances arisen over the vapor bubble surface in the condensing process is

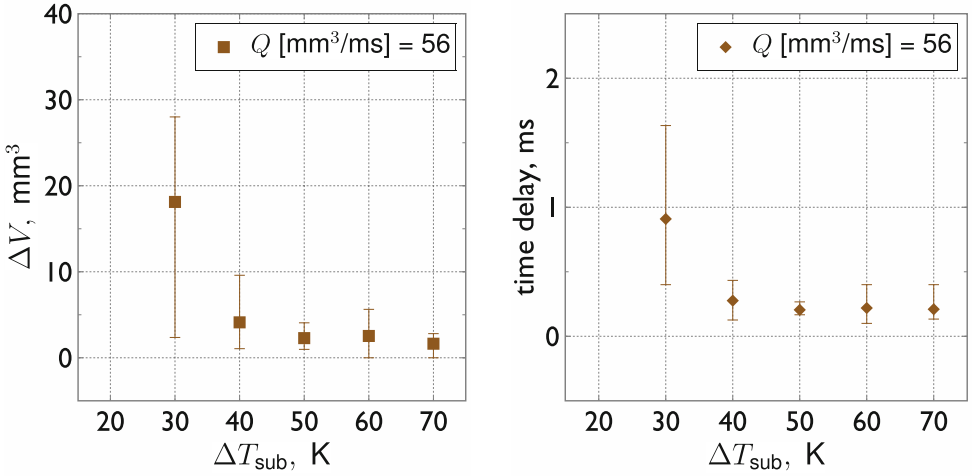

Fig. 7. (a) Volume variation ΔV and (b) time delay Δt against the degree of subcooling. The drop of the volume until the emergence of the disturbance is defined as $\Delta V = V_{\max} - V_{\mathrm{d}}$, and the time delay is defined as $\Delta t = t_{\mathrm{d}} - 0 = t_{\mathrm{d}}$, where V_{d} is the volume at $t = t_{\mathrm{d}}$, and t_{d} is the instance when the disturbances emerge on the bubble surface.

illustrated in Fig. 8 under $\Delta T_{\mathrm{sub}} = 40$ K. Noted that these images were taken in a different experimental run from those shown in Figs. 5 and 6. The first frame corresponds to the image at the instance when the bubble volume is almost maximum (defined as $t = t_1$). Shortly after that, the tiny disturbances emerge at the top of the bubble as indicated by arrows in the second frame (at $t = t_1 + 1/8$). As time elapses, the disturbances grow, and the number of the disturbances drastically increases over the interface by $t = t_1 + 3/8$. It is noted that the rest area of the bubble surface without the disturbances still remains smooth, and that the volume of the vapor bubble does not change apparently from $t = t_1$ to $t = t_1 + 3/8$. At $t = t_1 + 1/2$, ripples emerge over the rest area without disturbances, and one cannot see any smooth area over the free surface anymore. The volume of the bubble abruptly decreases at $t \geq t_1 + 1/2$ to result in collapse as shown in Fig. 5. In the case of the abrupt collapse under the $\Delta T_{\mathrm{sub}} \geq 30$ K, it is confirmed that the vapor bubble exhibits the variation of its morphology with such a scenario. In order to detect the trigger of the abrupt collapse, the wavelength of the fine disturbances is evaluated. We accumulate the size of the disturbances when the fine disturbances are recognized (corresponding to the instance at $t = t_1 + 1/8$ in Fig. 8), as the half of the wavelength of the instability. The wave number of the instability, $k = 1/\lambda$, when it emerges on the vapor bubble surface is plotted against the degree of subcooling, where λ is the wavelength of the instability. We measure the size of five to ten disturbances arisen over the free surface of a single vapor bubble, and accumulate the data for seven different bubbles under the same condition. It is noted that no fine disturbances are arisen under the conditions of $\Delta T_{\mathrm{sub}} \leq 20$ K. The wave number increases monotonically against ΔT_{sub} after the onset of the disturbances. Such trends of the characteristic wavenumber as well as the characteristic time of the collapse may be explained as follows by considering those experimental results. Before the pinch off the vapor bubble from the vapor, the injected vapor supplies heat to the vapor bubble interface, then the vapor bubble grows even in a rather high degree of subcooling. So that rather smooth interface maintains over the vapor bubble if the vapor column is still connected to the growing vapor bubble. After the pinch off of a vapor bubble from the vapor column injected,

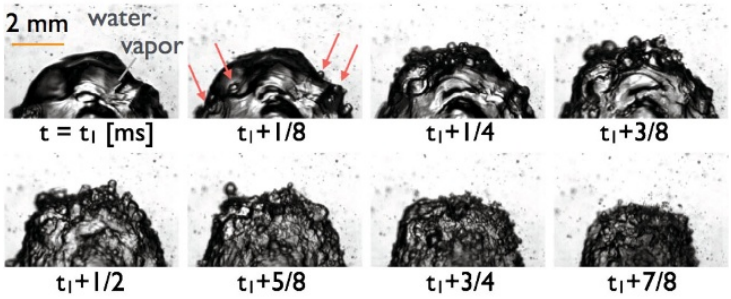

Fig. 8. Typical example of instability arisen in condensing process of the vapor bubble injected to the pool of 40 K in the degree of subcooling through the orifice. Arrows in the second frame indicate the fine disturbances of the free surface to result in the abrupt collapse of the vapor bubble. Scale bar in the first frame corresponds to 2.0 mm. Shutter speed is of 1/251,163 s.

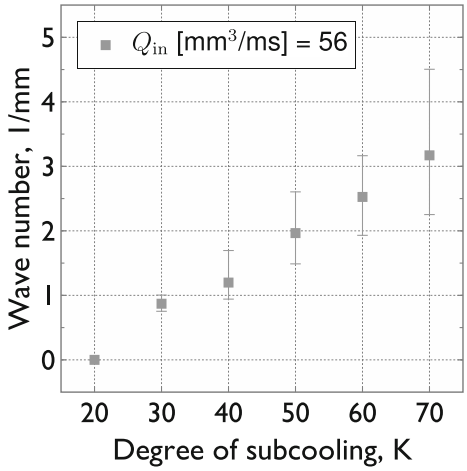

Fig. 9. Wave number of the instability when it emerges on the vapor bubble surface against the degree of subcooling.

supply of the heat due to the vapor injection to the vapor bubble interface is abruptly shut off. Then a breakage of the balance of the heat transfer between the vapor and the liquid through the vapor bubble interface takes place. Sudden condensation of the vapor near the interface leads an abrupt decrease of the pressure inside the bubble. Such a vigorous drop of the pressure inside the vapor bubble would result in the fine disturbances over the free surface. Amount of the vapor condensation must depend on the heat transfer between the vapor and the subcooled liquid (see Fig. 7), thus the pressure drop due to the abrupt condensation must become larger as ΔT_{sub}. As the degree of subcooling increases, the disturbance over the bubble becomes finer, and the characteristic time for the bubble collapse becomes shorter. Those disturbances over the bubble surface, in addition, result in the increase of the surface area to enhance the heat transfer through the vapor bubble surface. Such an increment of the vapor-liquid interface brings an acceleration of the condensation of the vapor in the bubble. Physical model of generating the interfacial instability on the condensing vapor bubble has not been comprehensively understood. Further researches are required to understand and to control the heat transfer accompanying the abrupt condensation of the vapor.

4 Concluding remarks

We focus on the growth/condensation processes of vapor bubble injected into a subcooled pool. We try to extract the vapor-liquid interaction by employing a vapor generator that supplies vapor at designated flow rate to the subcooled pool instead of using a immersed heating surface to realize a vapor bubble by general boiling phenomenon. We detect a spatio-temporal behavior of a single bubble of superheated vapor exposed to a subcooled liquid. We find that an abrupt condensation of the injected vapor results in fine disturbances over the vapor bubble surface before the collapse stage of the bubble. And, also find that such an instability arises slightly after the bubble size becomes maximum. We make a rough evaluation of the time series of the bubble volume by assuming that the vapor bubble is axisymmetric. It is found that the abrupt collapse of the vapor bubble is realized under the conditions of $R < 0$ and $\ddot{R} < 0$, where R is the corresponding "radius" to the evaluated volume ($R = \sqrt[3]{\frac{3V}{4\pi}}$). We evaluate the variation of the bubble volume as well as the period until the emergence of the disturbance as the trigger of the abrupt collapse the in order to understand the correlation between the fine disturbances over the free surface and the bubble behaviors in the condensing process. The wave number against the degree of subcooling is also illustrated.

This research is financially supported by the 45th Research Grant in Natural Sciences from The Mitsubishi Foundation (2014 – 2015). We gratefully acknowledge Prof. Masahiro Shoji (emeritus professor of The University of Tokyo and Kanagawa University) and his exstudents at Kanagawa University, Prof. Manabu Tange (Shibaura Institute of Technology), Mr. Makoto Watanabe (The University of Tokyo) and Prof. Koichi Suzuki (Tokyo University of Science, Yamaguchi) for fruitful discussion.

References

1. S. Inada, Y. Miyasaka, S. Sakamoto, G.R. Chandratilleke, J. Heat Trans. **108**, 219 (1986)
2. K. Suzuki, H. Saitoh, K. Matsumoto, Ann. N. Y. Acad. Sci. **974**, 364 (2002)
3. K. Suzuki, F. Inagaki, Proc. 5th Int. Conf. Enhanced, Compact and Ultra-compact Heat Exchangers: Science, Engineering and Technology **CD-ROM**, CHE2005 (2005)
4. K. Suzuki, F. Inagaki, I. Ueno, Trans. Japan Society for Aeronautical and Space Sciences (JSASS) Space Tech. Japan **7**, Ph67 (2009)
5. J. Tang, G. Zhu, L. Sun, Experimental Thermal and Fluid Science **50**, 97 (2013)
6. T. Saiki, T. Osawa, I. Ueno, C. Hong, Proc. ASME 2013 Int. Technical Conf. and Exhibition on Packing and Integration of Electronic and Photonic Microsystems (InterPACK2013), doi: 10.1115/IPACK2013–73153 (2013)
7. M. Tange, M. Yuasa, S. Takagi, M. Shoji, Proc. Microchannels and Minichannels 2004 (ICCM2004) (June 17–19, 2004, Rochester, New York, USA), p. 589 (2004)
8. G. Wang, P. Cheng, Int. J. Heat Mass Trans. **52**, 79 (2009)
9. J. Kim, J.F. Benton, D. Wisniewski, Int. J. Heat Mass Trans. **45**, 3919 (2002)
10. F. Demiray, J. Kim, Int. J. Heat Mass Trans. **47**, 3257 (2004)
11. T. Yabuki, T. Hamaguchi, O. Nakabeppu, J. Ther. Sci. Technol. **7**, 463 (2012)
12. D. Frost, B. Sturtevant, Phys. Fluids **29**, 2777 (1986)
13. C.E. Brennen, J. Fluid Mech. **472**, 153 (2002)
14. I. Ueno, M. Arima, Micrograv. Sci. Technol. **19**, 128 (2007)
15. I. Ueno, T. Saiki, T. Osawa, J. Ando, T. Kaneko, C. Hong, Proc. 15th International Heat Transfer Conference (IHTC-15), doi: 10.1615/IHTC15.pbl.009471 (2014)
16. K. Matsumoto, I. Ueno, J. Phys.: Conf. Ser. **147**, 012015 (2009)